Interference effects for the top quark decays $t \to b + W^+/H^+(\to \tau^+\nu_\tau)$

S. Mohammad Moosavi Nejad,[1,2,*] S. Abbaspour,[1] and R. Farashahian[1]

[1] *Faculty of Physics, Yazd University, P.O. Box 89195-741, Yazd, Iran*
[2] *School of Particles and Accelerators, Institute for Research in Fundamental Sciences (IPM), P.O.Box 19395-5531, Tehran, Iran*

(Received 5 March 2019; published 16 May 2019)

Applying the narrow-width approximation, we first review the next-to-leading-order QCD predictions for the total decay rate of a top quark considering two unstable intermediate particles: the W^+ boson in the standard model of particle physics and the charged Higgs boson H^+ in the generic type-I and -II two-Higgs-doublet models, i.e., $t \to b + W^+/H^+(\to \tau^+\nu_\tau)$. We then estimate the errors that arise from this approximation at leading-order perturbation theory. Finally, we investigate the interference effects in the factorization of production and decay parts of intermediate particles. We will show that for nearly mass-degenerate states ($m_{H^+} \approx m_{W^+}$) the correction due to the interference effect is considerable.

DOI: 10.1103/PhysRevD.99.095012

I. INTRODUCTION

Since the discovery in 1995 by the CDF and D0 experiments at the $p\bar{p}$ collider Tevatron at Fermilab, the top quark has been at or near the center of attention in high-energy physics. It is still the heaviest particle of the Standard Model (SM) of elementary particle physics, and its short lifetime implies that it decays before hadronization takes place. The remarkably large mass implies that the top quark couples strongly to the agents of electroweak symmetry breaking, making it both an object of interest itself and a tool to investigate that mechanism in detail.

The CERN LHC, producing a $t\bar{t}$ pair per second, is potentially a top quark factory which allows us to perform precision tests of the SM and will enhance the sensitivity of beyond-the-SM effects in the top sector. In this regard, a lot of theoretical work has gone into firming up the cross sections for the $t\bar{t}$ pair and the single top production at the Tevatron and the LHC, undertaken in the form of higher-order QCD corrections [1–4]. Historically, improved theoretical calculations of the top quark decay width and distributions started a long time ago. In this regard, the leading-order perturbative QCD corrections to the lepton energy spectrum in the decays $t \to bW^+ \to b(l^+\nu_l)$ were calculated some 30 years ago [5]. Subsequent theoretical works leading to analytic derivations implementing the $\mathcal{O}(\alpha_s)$ corrections were published in Refs. [6,7] and corrected in Ref. [8] (see also Refs. [9–11]). Moreover, in Refs. [12,13], the $\mathcal{O}(\alpha_s)$ radiative corrections to the decay rate of an unpolarized top quark are calculated, and the helicities of the W-gauge boson are specified as longitudinal, transverse plus, and transverse minus.

On the other hand, in the dominant decay mode $t \to bl^+\nu_l$, the bottom quark hadronizes into the b-jet X_b before it decays. Considering this hadronization process, in Ref. [13], the energy distribution of bottom-flavored hadrons (B mesons) inclusively produced in the SM decay chain of an unpolarized top quark, i.e., $t \to bW^+ \to Bl^+\nu_l + X$, is studied. In Refs. [14–17], the $\mathcal{O}(\alpha_s)$ angular distribution of the energy spectrum of hadrons considering the polar and azimuthal angular correlations in the rest frame decay of a polarized top quark, i.e., $t(\uparrow) \to B + W^+ + X$, is studied. Furthermore, the mass effects of quarks and hadrons have been also investigated.

Charged Higgs bosons emerge in the scalar sector of several extensions of the SM and are the object of various beyond SM (BSM) searches at the LHC. Since the SM does not include any elementary charged scalar particle, the experimental observation of a charged Higgs boson would necessarily be a signal for a nontrivially extended scalar sector and definitive evidence of new physics beyond the SM. In recent years, searches for charged Higgs have been done by the ATLAS and the CMS collaborations in proton-proton collision, and numerous attempts are still in progress at the LHC.

Among many proposed scenarios beyond the SM which motivate the existence of charged Higgs, a generic two-Higgs-doublet model (2HDM) [18–20] provides greater insight into the supersymmetry (SUSY) Higgs sector without including the plethora of new particles which SUSY predicts. Within this class of models, the Higgs sector of the

*mmoosavi@yazd.ac.ir

SM is extended by introducing an extra doublet of complex $SU(2)_L$ Higgs scalar fields. After spontaneous symmetry breaking, the two scalar Higgs doublets H_1 and H_2 yield three physical neutral Higgs bosons (h, H, and A) and a pair of charged-Higgs bosons ($H^\pm$) [19]. Moreover, after electroweak symmetry breaking, each doublet acquires a vacuum expectation value (VEV) $\mathbf{v}_i$ such that $\mathbf{v}_1^2+\mathbf{v}_2^2=(\sqrt{2}G_F)^{-1}$, where G_F is the Fermi constant and the $\mathbf{v}_1$ and $\mathbf{v}_2$ are the VEVs of H_1 and H_2, respectively. Furthermore, it is often useful to express the parameters $\tan\beta=\mathbf{v}_2/\mathbf{v}_1$ as the ratio of VEVs and the neutral sector mixing term $\sin(\beta-\alpha)$. In fact, the angles α and β govern the mixing between mass eigenstates in the CP-even sector and CP-odd/charged sectors, respectively.

The dominant production and decay modes for a charged Higgs boson depend on the value of its mass with respect to the top quark mass and can be classified into three categories [21]. Among them, light charged Higgs scenarios are defined by Higgs-boson masses smaller than the top quark mass. In the 2HDM, the main production mode for light charged Higgses is through the top quark decay $t\to bH^+$. Therefore, at the CERN LHC, the light Higgses can be searched in the subsequent decay products of the top pairs $t\bar{t}\to H^\pm H^\mp b\bar{b}$ and $t\bar{t}\to H^\pm W^\mp b\bar{b}$ when charged Higgs decays into the τ lepton and neutrino. In Refs. [22,23], the $\mathcal{O}(\alpha_s)$ QCD corrections to the hadronic decay width of a charged Higgs boson, i.e., $\Gamma(t\to bH^+)$, are calculated, and in Ref. [24], the leading-order contribution and the $\mathcal{O}(\alpha_s)$ corrections to the polarized top quark decay into bH^+ are computed. In Refs. [25,26], the energy distribution of B hadrons is investigated in the unpolarized top decays through the 2HDM scenarios, i.e., $t\to bH^+\to BH^+ +\text{jets}$. In Ref. [27], in the 2HDM framework, the $\mathcal{O}(\alpha_s)$ angular distribution of the energy spectrum of B/D mesons is studied by considering the polar and the azimuthal angular correlations in the rest frame decay of a polarized top quark, i.e., $t(\uparrow)\to B/D+H^+ + X$ followed by $H^+\to l^+\nu_l$. Note that, even though current ATLAS and CMS measurements exclude a light charged Higgs for most of the parameter regions in the context of the minimal supersymmetric standard model (MSSM) scenarios, these bounds are significantly weakened in the type-II 2HDM (MSSM) once the exotic decay channel into a lighter neutral Higgs, $H^\pm\to AW^\pm/HW^\pm$, is open. In Ref. [28], the production possibility of a light charged Higgs in top quark decay via single top or top pair production is examined, with a subsequent decay as $H^\pm\to AW^\pm/HW^\pm$. It is shown that this decay mode can reach a sizable branching fraction at low $\tan\beta$ once it is kinematically permitted. These results show that the exotic decay channel $H^+\to AW^+/HW^+$ is complementary to the conventional $H^+\to\tau^+\nu_\tau$ channel considered in the current MSSM scenarios.

Two considerable points about all mentioned works are as follows. First, in all works, authors have applied the narrow width approximation (NWA) in which an intermediate gauge boson (W^+ boson in the SM and H^+ boson in the 2HDM scenario) is considered the on-shell particle. Second, the contribution of the interference term in the total decay rate of top quarks is ignored. In this work, we shall examine how much these two approximations change the results. Note that an important condition limiting the applicability of the narrow width approximation, however, is the requirement that there should be no interference of the contribution of the intermediate particle for which the NWA is applied with any other close-by resonance. It should be noted that, in a general case, if the mass gap between two intermediate particles is smaller than one of their total widths, the interference term between the contributions from the two nearly mass-degenerate particles may become large. In these cases, a single resonance approach or the incoherent sum of the contributions due to two resonances does not necessarily hold.

This work is organized as follows. In Sec. II, we calculate the Born rate of top quark decay in the SM through the direct approach and the narrow width approximation. We will also present the next-to-leading-order (NLO) QCD corrections to the tree-level rate of top decay. In Sec. III, the same calculations will be done by working in the general 2HDM. In Sec. IV, we present our results for the interference effects on the total top quark decay and show when this effect is considerable. In Sec. V, we summarize our conclusions.

II. TOP QUARK DECAY IN THE SM $t\to bW^+\to bl^+\nu_l$

For the Cabibbo-Kobayashi-Maskawa quark mixing matrix [29], one has $|V_{tb}|\approx 1$. Therefore, the top quark decays within the SM are completely dominated by the mode $t\to bW^+$ followed by $W^+\to l^+\nu_l$ where $l^+=e^+,\mu^+,\tau^+$. Since the top quark's lifetime is much shorter than the typical strong interaction time, the top quark decay dynamics is controlled by the perturbation theory. Therefore, incorporating the QED/QCD perturbative corrections, one has precise theoretical predictions for the decay width to be confronted with the experimental data. For a warm-up exercise, we start to calculate the decay width of the process

$$t(p_t)\to b(p_b)+W^+(p_W)\to b(p_b)+l^+(p_l)+\nu_l(p_\nu) \tag{1}$$

at the Born approximation. The matrix element of this process at tree level is given by

$$\begin{aligned}M_{\text{Born}}^{\text{SM}}\equiv M_0^{\text{SM}}=-\frac{g_W^2}{8}|V_{tb}|\left(\frac{-g^{\alpha\beta}+\frac{p_W^\alpha p_W^\beta}{m_W^2}}{p_W^2-m_W^2}\right)\\ \times[\bar{u}_b(p_b)\gamma_\alpha(1-\gamma_5)u_t(p_t)]\\ \times[\bar{u}_\nu(p_\nu)\gamma_\beta(1-\gamma_5)v_l(p_l)],\end{aligned} \tag{2}$$

where $g_W^2 = 4\pi\alpha/\sin^2\theta_W = 8m_W^2 G_F/\sqrt{2}$ is the electroweak coupling constant, θ_W is the weak mixing angle, and m_W is the W^+-boson mass. Since the second term in parentheses (2) is proportional to the lepton mass due to the conservation of the lepton current, it can be omitted simply. Therefore, the matrix element squared reads

$$|M_0^{\rm SM}(t\to bl^+\nu_l)|^2 = \left(\frac{2g_W^2|V_{tb}|}{p_W^2-m_W^2}\right)^2 (p_b\cdot p_\nu)(p_l\cdot p_t), \quad (3)$$

where, for the convenient scalar products in the top quark rest frame, one has $2p_b\cdot p_\nu = m_t^2+m_l^2-m_b^2-2m_tE_l$ and $p_t\cdot p_l = m_tE_l$, in which E_l is the energy of the lepton in the top quark rest frame. Technically, to obtain the matrix element squared for the polarized top decay, one should replace $\sum_{s_t} u(p_t,s_t)\bar{u}(p_t,s_t) = (\not{p}_t+m_t)$ in the unpolarized Dirac string by $u(p_t,s_t)\bar{u}(p_t,s_t) = (1-\gamma_5\not{s}_t)(\not{s}_t+m_t)/2$.

Since the main contribution to the top quark decay mode (1) comes from the kinematic region where the W^+ boson is near its mass shell, one has to take into account its finite decay width Γ_W. For this reason, in Eq. (3), we employ the Breit-Wigner prescription of the W^+-boson propagator for which the propagator contribution of an unstable particle of mass M_W and total width Γ_W is given by

$$\frac{1}{p_W^2-M_W^2} \to \frac{1}{p_W^2-M_W^2+iM_W\Gamma_W}. \quad (4)$$

Thus, the matrix element squared (3) reads

$$|M_0^{\rm SM}(t\to bl^+\nu_l)|^2 = \frac{g_W^4 m_t^3|V_{tb}|^2}{(p_W^2-m_W^2)^2+m_W^2\Gamma_W^2} \times E_l\left\{1+\left(\frac{m_l}{m_t}\right)^2-\left(\frac{m_b}{m_t}\right)^2-\frac{2E_l}{m_t}\right\}. \quad (5)$$

The phase space element for the three particles final state is given by

$$dPS_3 = (2\pi)^{-5}\frac{d^3\vec{p}_b}{2E_b}\frac{d^3\vec{p}_\nu}{2E_\nu}\frac{d^3\vec{p}_l}{2E_l}\delta^4(p_t-p_b-p_\nu-p_l) = \frac{1}{2^5\pi^3}dE_b dE_l. \quad (6)$$

Ignoring the lepton mass ($m_l\approx 0$), the kinematic restrictions are $m_t/2-E_l\le E_b\le m_t/2$ and $0\le E_l\le m_t/2(1-(m_b/m_t)^2)$, where E_b is the energy of the b quark. For the Born decay width, we use Fermi's golden rule

$$d\Gamma_0 = \frac{1}{2m_t}\overline{|M_0|^2}dPS_3, \quad (7)$$

where $\overline{|M_0|^2} = \sum_{\rm spin}|M_0|^2/(1+2s_t)$ and s_t stands for the top quark spin. Thus, for the case of unpolarized top quark decay, we obtain the decay rate at the lowest order as

$$\begin{aligned}\Gamma_0^{\rm SM}(t\to bl^+\nu_l) = \frac{m_t\alpha^2|V_{tb}|^2}{192\pi\sin^4\theta_W}\Bigg\{&2(R-1)(1+R-2\omega)+\left[3(\omega-1)(R-\omega)+\omega\frac{\Gamma_W^2}{m_t^2}\right]\ln\frac{\omega\Gamma_W^2+m_t^2(R-\omega)^2}{\omega\Gamma_W^2+m_t^2(1-\omega)^2}\\ &+\frac{1}{m_t\sqrt{\omega}\Gamma_W}[3\omega\Gamma_W^2(1+R-2\omega)+m_t^2(1-R)^3+m_t^2(R-\omega)^2(R+2\omega-3)]\\ &\times\left(\tan^{-1}\frac{m_t(\omega-R)}{\sqrt{\omega}\Gamma_W}+\tan^{-1}\frac{m_t(1-\omega)}{\sqrt{\omega}\Gamma_W}\right)\Bigg\}, \end{aligned} \quad (8)$$

where we defined $R=(m_b/m_t)^2$ and $\omega=(m_W/m_t)^2$. Concentrating on the case $l^+\nu_l=\tau^+\nu_\tau$ with $m_\tau = 1.776$ GeV and taking $m_t = 172.98$ GeV, $m_W = 80.339$ GeV, $m_b = 4.78$ GeV, $\Gamma_W = 2.085\pm 0.042$ GeV, $\sin^2\theta_W = 0.2312$, $\alpha = 0.0077$, and $|V_{tb}|\approx 1$ [30], one has

$$\Gamma_0^{\rm SM}(t\to b\tau^+\nu_\tau) = 0.1543. \quad (9)$$

Extension of this approach to higher orders of perturbative QED/QCD is complicated. For example, at the NLO perturbative QCD, the phase space element contains four particles, including a real emitted gluon, so this leads to cumbersome computations. For this reason, in all manuscripts, authors have applied the narrow width approximation, which will be described in the following.

A. Narrow width approximation

The separation of a more complicated process into several subprocesses involving on-shell incoming and outgoing particles is achieved with the help of the NWA. This approximation is based on the observation that the on-shell contribution is strongly enhanced if the total width is much smaller than the mass of the particle, i.e., $\Gamma \ll M$. Here, we briefly describe how the NWA works for the decay process of the top quark.

On squaring the Born matrix element (2) and taking the Breit-Wigner prescription, one is led to the Born contribution

$$|M_0^{\rm SM}|^2 = \frac{1}{(p_W^2-m_W^2)^2+(m_W\Gamma_W)^2} \times|M^{\rm Born}(t\to bW^+)|^2|M^{\rm Born}(W^+\to l^+\nu_l)|^2, \quad (10)$$

where $|M^{\rm Born}(t\to bW^+)|^2 = 2g_W^2|V_{tb}|^2(p_b\cdot p_t)$ and $|M^{\rm Born}(W^+\to l^+\nu_l)|^2 = 2g_W^2(p_l\cdot p_\nu)$. We now factorize the three-body decay rate (6) into the two-body rates $\Gamma(t\to bW^+)$ and $\Gamma(W^+\to l^+\nu_l)$ using the NWA for the W^+ boson for which the condition $\Gamma_W \ll m_W$ holds. First, we introduce the identity

$$1 = \int dp_W^2 \int \frac{d^3p_W}{2E_W}\delta^4(p_{W^+} - p_{l^+} - p_{\nu_l}); \qquad (11)$$

therefore, the decay rate (7) reads

$$d\Gamma_0 = 2m_W \int \frac{dp_W^2}{2\pi}\overline{|M_0^{\rm SM}|^2} \times \frac{1}{2m_t}\overbrace{\left\{\frac{d^3p_b}{(2\pi)^3 2E_b}\frac{d^3p_W}{(2\pi)^3 2E_W}(2\pi)^4\delta^4(p_t - p_b - p_{W^+})\right\}}^{dPS_2(t\to bW^+)} \times \frac{1}{2m_W}\underbrace{\left\{\frac{d^3p_l}{(2\pi)^3 2E_l}\frac{d^3p_{\nu_l}}{(2\pi)^3 2E_{\nu_l}}(2\pi)^4\delta^4(p_{W^+} - p_{l^+} - p_{\nu_l})\right\}}_{dPS_2(W^+\to l^+\nu_l)}. \qquad (12)$$

Next, the phase space is nicely factorized so that by substituting $|M_0^{\rm SM}|^2$ (10) one finds

$$d\Gamma_0 = \frac{m_W}{\pi}\int dp_W^2 \frac{1}{(p_W^2 - m_W^2)^2 + (m_W\Gamma_W)^2} \times \left\{\frac{1}{2m_t}[\overline{|M^{\rm Born}_{t\to bW^+}|^2}]dPS_2(t\to bW^+) \times \frac{1}{2m_W}[\overline{|M^{\rm Born}_{W^+\to l^+\nu_l}|^2}]dPS_2(W^+\to l^+\nu_l)\right\}. \qquad (13)$$

Adopting the NWA approach, the Breit-Wigner resonance is replaced by a delta function as [31]

$$\frac{1}{(p_W^2 - m_W^2)^2 + (m_W\Gamma_W)^2} \approx \frac{\pi}{m_W\Gamma_W}\delta(p_W^2 - m_W^2). \qquad (14)$$

This approximation is expected to work reliably up to terms of $\mathcal{O}(\Gamma_W/m_{W^+})$. As was discussed, a necessary condition limiting the applicability of this approximation is the requirement that there should be particles with a total decay width much smaller than their mass; otherwise, the integral (13) is reduced to [31]

$$\int dp_W^2 \frac{1}{(p_W^2 - m_W^2)^2 + (m_W\Gamma_W)^2} = -\frac{1}{m_W\Gamma_W}\tan^{-1}\left[\frac{m_W^2 - p_W^2}{m_W\Gamma_W}\right]. \qquad (15)$$

Using the NWA, the three-body decay $t\to b\tau^+\nu_\tau$ is factorized as

$$\Gamma(t\to bl^+\nu_l) = \Gamma(t\to bW^+)\frac{\Gamma(W^+\to l^+\nu_l)}{\Gamma_W} = \Gamma(t\to bW^+){\rm Br}(W^+\to l^+\nu_l), \qquad (16)$$

which is a result expected from physical intuition and is expected to work reliably up to terms of $\mathcal{O}(\Gamma_W/m_{W^+})$. For three individual leptonic branching ratios, one has ${\rm Br}(W^+\to e^+\nu_e) = 10.75\pm 0.13$, ${\rm Br}(W^+\to \mu^+\nu_\mu) = 10.57\pm 0.15$ and ${\rm Br}(W^+\to \tau^+\nu_\tau) = 11.25\pm 0.20$ in units 10^{-2} [32].

In (16), the partial Born width of the decay $t\to bW^+$ differential in the angle θ_P enclosed between the top quark polarization 3-vector $\vec{P}$ and the bottom quark 3-momentum $\vec{p}_b$ is given by [14,16]

$$\frac{d\Gamma_0^{\rm SM}}{d\cos\theta_P}(t\to bW^+) = \frac{1}{2}(\Gamma_0^{\rm SM} + P\Gamma_{0P}^{\rm SM}\cos\theta_P), \qquad (17)$$

where $P = |\vec{P}|(0\le P\le 1)$ is the degree of polarization and

$$\Gamma_0^{\rm SM} = \frac{m_t\alpha\sqrt{S^2 - R}}{8\sin^2\theta_W}\left(1 + R - 2\omega + \frac{(1-R)^2}{\omega}\right),$$
$$\Gamma_{0P}^{\rm SM} = \frac{m_t\alpha}{4\omega\sin^2\theta_W}(1 - R - 2\omega)(S^2 - R). \qquad (18)$$

Here, we defined $S = (1 + R - \omega)/2$. Taking the input parameters as before, one has

$$\Gamma_0^{\rm SM}(t\to bW^+) = 1.463,$$
$$\Gamma_{0P}^{\rm SM}(t(\uparrow)\to bW^+) = 0.579. \qquad (19)$$

Considering the factorization (16), one has $\Gamma_0^{\rm SM}(t\to b\tau^+\nu_\tau) = 1.463\times{\rm Br}(W^+\to\tau^+\nu_\tau) = 0.1645$, which is in agreement with the result obtained in the full calculation (9) up to the accuracy about 5%. One also has $\Gamma_0^{\rm SM}(t\to b\mu^+\nu_\mu) = 0.1543$ and $\Gamma_0^{\rm SM}(t\to be^+\nu_e) = 0.1569$.

In Ref. [13], we have calculated the NLO QCD corrections to the differential decay rate of $t\to bW^+$ in the massless (with $m_b = 0$) and massive (with $m_b \neq 0$) schemes. The result for the massless decay rate reads

$$\Gamma^{\rm SM}_{\rm NLO}(t\to bW^+) = \Gamma^{\rm SM}_0\bigg\{1+\frac{C_F\alpha_s}{2\pi}\bigg[-\frac{2\pi^2}{3}-4Li_2(\omega)-\frac{5+4\omega}{1+2\omega}\ln(1-\omega) -2\frac{\omega(1+\omega)(1-2\omega)}{(1-\omega)^2(1+2\omega)}\ln\omega-2\ln\omega\ln(1-\omega) -\frac{1+3(1+2\omega)(\omega-2)}{2(1-\omega)(1+2\omega)}\bigg]\bigg\}. \tag{20}$$

In Ref. [13], using the NWA approach, we have also calculated the NLO QCD corrections to the differential decay rate of $t\to bW^+\to bl^+\nu_l$ considering the helicity contributions of the W^+ boson. In Refs. [15–17], we have computed the differential decay width for the process $t(\uparrow)\to bW^+$ up to the NLO accuracy. Our numerical results read

$$\begin{aligned}\Gamma^{\rm SM}_{\rm NLO}(t\to bW^+) &= \Gamma^{\rm SM}_0(1-0.0853),\\ \Gamma^{\rm SM}_{\rm NLO,P}(t(\uparrow)\to bW^+) &= \Gamma^{\rm SM}_{0P}(1-0.1308).\end{aligned} \tag{21}$$

Thus, the $\mathcal{O}(\alpha_s)$ contribution to the unpolarized and polarized top width is -8.53% and -13%, respectively, while the contribution of the finite W-width effect is about 5%. It should be noted that the $\mathcal{O}(\alpha)$ electroweak corrections contribute typically by $+1.55\%$ [33,34].

III. TOP QUARK DECAY IN THE 2HDM

In the theories beyond the SM with an extended Higgs sector one may also have the decay mode

$$t\to bH^+\to bl^+\nu_l, \tag{22}$$

provided that $m_t > m_{H^+}+m_b$. A model-independent lower bound on the Higgs mass m_{H^+} arising from the nonobservation of the charged Higgs pair production at LEPII has yielded $m_{H^\pm} > 79.3$ GeV at 95% C.L. [35]. As is asserted in Ref. [36], a charged Higgs with a mass in the range $80\le m_{H^\pm}\le 160$ GeV is a logical possibility, and its effect should be searched for in the process (22). A beginning along these lines has already been done at the Tevatron [37,38], but a definitive search of the charged Higss bosons over a good part of the $(m_{H^\pm}-\tan\beta)$ plane is a plan which still has to be done, and this belongs to the CERN LHC experiments [39].

Here, we review some technical details about the decay rate of the unpolarized top quark in the process (22) by working in the general 2HDM [18–20] in which H_1 and H_2 are the doublets of which the VEVs give masses to the down- and up-type quarks. Moreover, a linear combination of the charged components of doublets H_1 and H_2 gives two physical charged Higgs bosons $H^\pm$, i.e., $H^\pm = H_2^\pm\cos\beta - H_1^\pm\sin\beta$.

In a general 2HDM, in order to avoid tree-level flavor-changing neutral currents, which can be induced by Higgs exchange, the generic Higgs-boson coupling to all types of quarks must be restricted. Fortunately, there are several classes of two-Higgs-doublet models which naturally avoid this difficulty by restricting the Higgs coupling. Imposing flavor conservation, there are four possibilities (models I–IV) for the two Higgs doublets to couple to the SM fermions so that each gives rise to rather different phenomenology predictions. In these four models, assuming massless neutrinos, the generic charged Higgs coupling to the SM fermions can be expressed as a superposition of right- and left-chiral coupling factors [40], so the relevant part of the interaction Lagrangian of the process (22) is given by

$$\begin{aligned}L_I = \frac{g_W}{2\sqrt{2}m_W}H^+\{&V_{tb}[\bar{u}_t(p_t)\{A(1+\gamma_5)\\ &+B(1-\gamma_5)\}u_b(p_b)]\\ &+C[\bar{u}_{\nu_l}(p_\nu)(1-\gamma_5)u_l(p_l)]\},\end{aligned} \tag{23}$$

where A, B, and C are three model-dependent parameters.

In the first possibility (called model I), the H_2 doublet gives masses to all quarks and leptons, so the other one, i.e., doublet H_1, essentially decouples from fermions. In this model, one has

$$A_{\rm I}=m_t\cot\beta,\quad B_{\rm I}=-m_b\cot\beta,\quad C_{\rm I}=-m_\tau\cot\beta. \tag{24}$$

In the second scenario (called model II), the H_2 doublet gives mass to the right-chiral up-type quarks (and possibly neutrinos), and the H_1-doublet gives mass to the right-chiral down-type quarks and charged leptons. In this possibility, the Lagrangian (23) contains

$$A_{\rm II}=m_t\cot\beta,\quad B_{\rm II}=m_b\tan\beta,\quad C_{\rm II}=m_\tau\tan\beta. \tag{25}$$

There are also two other scenarios (models III and IV) in which the down-type quarks and charged leptons receive masses from different doublets; in model III, both up- and down-type quarks couple to the second doublet (H_2), and all leptons couple to the first one, so one has

$$A_{\rm III}=m_t\cot\beta,\quad B_{\rm III}=m_b\tan\beta,\quad C_{\rm III}=-m_\tau\cot\beta, \tag{26}$$

and in the fourth scenario (model IV), the roles of two doublets are reversed with respect to model II, i.e.,

$$A_{\rm IV}=m_t\cot\beta,\quad B_{\rm IV}=-m_b\cot\beta,\quad C_{\rm IV}=m_\tau\tan\beta. \tag{27}$$

These four models are also known as type I-IV 2HDM scenarios. Note that the type-II scenario is, in fact, the Higgs sector of the MSSM up to SUSY corrections [41,42]. In other words, in the MSSM, we have a type-II 2HDM sector in addition to the supersymmetric particles including the stops, charginos, and gluinos.

After this description, we start to calculate the Born term contribution to the decay rate of the process $t\to bl^+\nu_l$ ($l^+=e^+,\mu^+,\tau^+$). Considering the decay process

$$t(p_t) \to b(p_b) + H^+(p_{H^+}) \to b(p_b) + l^+(p_l) + \nu_l(p_\nu) \tag{28}$$

and using the couplings from the Lagrangian (23), one can write the matrix element of the process (28) as

$$M_0^{\rm BSM}(t \to bl^+\nu_l) = \frac{g_W^2|V_{tb}|}{8m_W^2}\frac{1}{p_{H^+}^2 - m_{H^+}^2 + im_{H^+}\Gamma_H}C[\bar{u}_\nu(p_\nu)(1+\gamma_5)v_l(p_l)][\bar{u}_b(p_b)\{A(1+\gamma_5)+B(1-\gamma_5)\}u_t(p_t)]. \tag{29}$$

Thus, the matrix element squared reads

$$|M_0^{\rm BSM}(t \to bl^+\nu_l)|^2 = \left(\frac{g_W^2|V_{tb}|}{\sqrt{2}m_W^2}\right)^2 \frac{1}{[p_{H^+}^2 - m_{H^+}^2]^2 + m_{H^+}^2\Gamma_H^2} C^2(p_l \cdot p_\nu)\{(A^2+B^2)p_b \cdot p_t + 2m_b m_t AB\}. \tag{30}$$

The kinematic restrictions and the phase space element are as before; see Eq. (6). Thus, defining $y = (m_{H^+}/m_t)^2$, for the unpolarized decay rate, one has

$$\begin{aligned}\Gamma_0^{\rm BSM}(t \to bl^+\nu_l) = {}& \left(\frac{C\alpha|V_{tb}|}{16\sqrt{\pi}m_W^2\sin^2\theta_W}\right)^2 \times \Bigg\{ m_t(R-1)[8AB\sqrt{R} + (A^2+B^2)(3+R-4y)] \\ & + 2\frac{\sqrt{y}}{\Gamma_H}\left(\tan^{-1}\frac{m_t(y-R)}{\sqrt{y}\Gamma_H} + \tan^{-1}\frac{m_t(1-y)}{\sqrt{y}\Gamma_H}\right)[4AB\sqrt{R}(\Gamma_H^2 + (1-y)m_t^2) \\ & + (A^2+B^2)[(2+R-3y)\Gamma_H^2 + m_t^2(1-y)(1+R-y)]] \\ & + m_t\left[4AB(2y-1)\sqrt{R} + (A^2+B^2)\left(\frac{y\Gamma_H^2}{m_t^2} - (1+R-4y-2Ry+3y^2)\right)\right] \times \ln\frac{y\Gamma_H^2 + m_t^2(R-y)^2}{y\Gamma_H^2 + m_t^2(1-y)^2}\Bigg\}. \end{aligned} \tag{31}$$

Leaving this result and working in the NWA framework, in which $p_{H^+}^2 = m_{H^+}^2$ is given from the beginning, we have

$$\Gamma_0^{\rm BSM}(t \to bl^+\nu_l) = \Gamma_0(t \to bH^+) \times {\rm Br}(H^+ \to l^+\nu_l), \tag{32}$$

where ${\rm Br}(H^+ \to l^+\nu_l) = \Gamma_0(H^+ \to l^+\nu_l)/\Gamma_H^{\rm Total}$, and the polarized and unpolarized tree-level decay widths read [25–27]

$$\begin{aligned}\Gamma_0^{\rm BSM}(t \to bH^+) &= \frac{m_t}{16\pi}\{(a^2+b^2)(1+R-y) + 2(a^2-b^2)\sqrt{R}\}\lambda^{\frac{1}{2}}(1,R,y), \\ \Gamma_{0P}^{\rm BSM}(t(\uparrow) \to bH^+) &= \frac{m_t}{8\pi}(ab)\lambda(1,R,y). \end{aligned} \tag{33}$$

Here, $\lambda(x,y,z) = (x-y-z)^2 - 4yz$ is the Källén function (triangle function), and, for simplicity, we introduced the coefficients a and b as

$$\begin{aligned} a &= \frac{g_W}{2\sqrt{2}m_W}|V_{tb}|(A+B), \\ b &= \frac{g_W}{2\sqrt{2}m_W}|V_{tb}|(A-B), \\ c &= \frac{g_W}{2\sqrt{2}m_W}C. \end{aligned} \tag{34}$$

The advantage of this notation is that the coupling of the charged Higgs to the bottom and top quarks is expressed as a superposition of scalar and pseudoscalar coupling factors. The NLO QCD radiative corrections to the polarized and unpolarized rates are given in our previous works [25–27].

Since all current search strategies postulate that the charged Higgs decays either leptonically ($H^+ \to \tau^+\nu_\tau$) or hadronically ($H^+ \to c\bar{s}$), we adopt, following Ref. [43], the relevant branching fraction ${\rm Br}(H^+ \to \tau^+\nu_\tau)$ as

$${\rm Br}(H^+ \to \tau^+\nu_\tau) = \frac{\Gamma(H^+ \to \tau^+\nu_\tau)}{\Gamma(H^+ \to \tau^+\nu_\tau) + \Gamma(H^+ \to c\bar{s})}, \tag{35}$$

where in model I (and IV) one has

$$\begin{aligned}\Gamma_0(H^+ \to \tau^+\nu_\tau) &= \frac{g_W^2 m_{H^+}}{32\pi m_W^2}m_\tau^2\cot^2\beta, \\ \Gamma(H^+ \to c\bar{s}) &= \frac{3g_W^2 m_{H^+}}{32\pi m_W^2}|V_{cs}|^2(\cot^2\beta)\lambda^{\frac{1}{2}}\left(1, \frac{m_c^2}{m_{H^+}^2}, \frac{m_s^2}{m_{H^+}^2}\right)\left[(m_c^2+m_s^2)\left(1 - \frac{m_c^2}{m_{H^+}^2} - \frac{m_s^2}{m_{H^+}^2}\right) + 4\frac{m_c^2 m_s^2}{m_{H^+}^2}\right] \end{aligned} \tag{36}$$

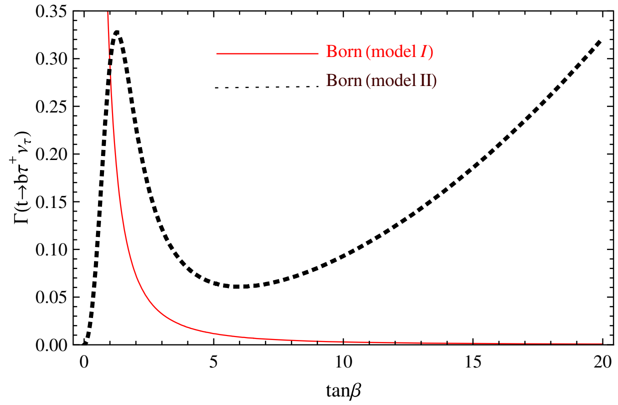

FIG. 1. The Born decay rate of $t \to b\tau^+\nu_\tau$ as a function of $\tan\beta$ in two scenarios for which $m_{H^+} = m_{W^+}$ is set.

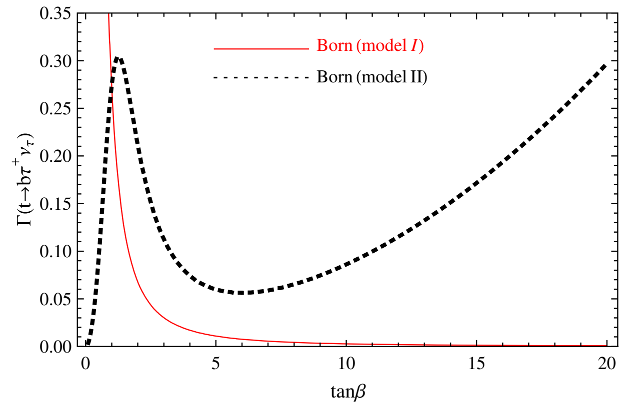

FIG. 2. As in Fig. 1 but for $m_{H^+} = 85$ GeV.

and for model II (and III) one has

$$\Gamma_0(H^+ \to \tau^+\nu_\tau) = \frac{g_W^2 m_{H^+}}{32\pi m_W^2} m_\tau^2 \tan^2\beta,$$
$$\Gamma(H^+ \to c\bar{s}) = \frac{3g_W^2 m_{H^+}}{32\pi m_W^2}|V_{cs}|^2 \lambda^{\frac{1}{2}}\left(1, \frac{m_c^2}{m_{H^+}^2}, \frac{m_s^2}{m_{H^+}^2}\right) \times \left[(m_c^2\cot^2\beta + m_s^2\tan^2\beta) \times \left(1 - \frac{m_c^2}{m_{H^+}^2} - \frac{m_s^2}{m_{H^+}^2}\right) - 4\frac{m_c^2 m_s^2}{m_{H^+}^2}\right]. \quad (37)$$

Both results are in complete agreement with Ref. [22].

In the limit of $m_i^2/m_H^2 \to 0$ $(i = c, s)$, the branching fraction (35) in the type-I 2HDM is simplified as

$$\mathrm{Br}(H^+ \to \tau^+\nu_\tau) = \frac{1}{1 + 3|V_{cs}|^2[(\frac{m_s}{m_\tau})^2 + (\frac{m_c}{m_\tau})^2]}, \quad (38)$$

which is independent of the $\tan\beta$ and in the type-II reads

$$\mathrm{Br}(H^+ \to \tau^+\nu_\tau) = \frac{1}{1 + 3|V_{cs}|^2[(\frac{m_s}{m_\tau})^2 + (\frac{m_c}{m_\tau})^2\cot^4\beta]}. \quad (39)$$

Taking $m_s = 95$ MeV, $m_c = 1.67$ GeV, $m_\tau = 1.776$ GeV, and $|V_{cs}| = 0.9734$, the branching ratio in model I reads $\mathrm{Br} = 0.284$. While in model I the branching ratio is independent of the $\tan\beta$, in the type-II scenario, it depends on the $\tan\beta$. It is simple to prove that for $\tan\beta > 5$ one has $\mathrm{Br} \approx 1$ in model II to a very high accuracy. Direct searches at the LHC, with the center-of-mass energy of 7 [44–46] and 8 TeV [47,48] set stringent constraints on the $m_{H^\pm} - \tan\beta$ parameter space.

Taking $m_{H^+} = 95$ GeV and $\tan\beta = 8$, from full calculation (31), one has $\Gamma_0^{\mathbf{Model\,I}} = 36 \times 10^{-4}$ in the type-I 2HDM, while the corresponding result in the type-II 2HDM reads $\Gamma_0^{\mathbf{Model\,II}} = 559 \times 10^{-4}$. Considering Eqs. (32)–(39), our results in the NWA scheme read $\Gamma_0^{\mathbf{Model\,I}} = 35 \times 10^{-4}$ and $\Gamma_0^{\mathbf{Model\,II}} = 568 \times 10^{-4}$. As is seen, the results (31) obtained through the direct approach are in good agreement with the ones from the NWA for both models up to the accuracies about 1.6% (for model I) and 2.7% (for model II).

Applying Eq. (31), in Figs. 1–3, we studied the dependence of the top quark decay rate on $\tan\beta$ considering $m_{H^+} = m_{W^+}$ (in Fig. 1), $m_{H^+} = 85$ GeV (in Fig. 2), and $m_{H^+} = 120$ GeV (in Fig. 3). As is seen, for $\tan\beta > 2$, the Born rate in model II is always larger than the one in model I, and the lowest value at the type-II model occurs at $\tan\beta = 6$. From Fig. 1, it can be also seen that for $m_{H^+} = m_{W^+}$ one has $\Gamma_0^{\mathbf{Model\,II}} \geq \Gamma_0^{\mathrm{SM}} (= 0.1543)$ when $\tan\beta > 14$ is considered. In Figs. 4 and 5, varying the charged Higgs-boson mass, we investigated the behavior of the top decay rate at the Born level for both models when $\tan\beta$ is fixed. In Ref. [26], we have calculated the QCD corrections to the differential decay rate of $t \to bH^+$ up to NLO accuracy. Taking $m_{H^+} = m_{W^+}$ and $\tan\beta = 8$, one has

$$\Gamma_{\mathrm{NLO}}^{\mathbf{Model\,I}}(t \to bH^+) = \Gamma_0^{\mathbf{Model\,I}}(1 - 0.0879),$$
$$\Gamma_{\mathrm{NLO}}^{\mathbf{Model\,II}}(t \to bH^+) = \Gamma_0^{\mathbf{Model\,II}}(1 - 0.4635), \quad (40)$$

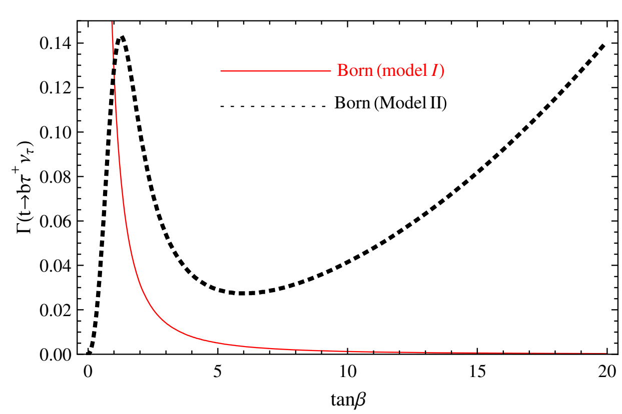

FIG. 3. As in Fig. 1 but for $m_{H^+} = 120$ GeV.

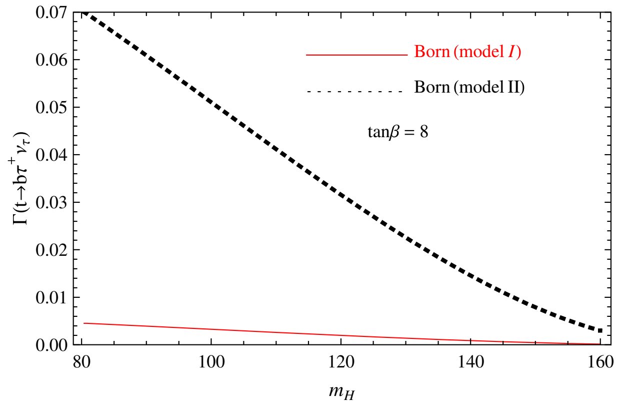

FIG. 4. $\Gamma^{\rm BSM}_{\rm Born}(t \to b\tau^+\nu_\tau)$ as a function of m_{H^+} in two scenarios for which $\tan\beta = 8$ is set.

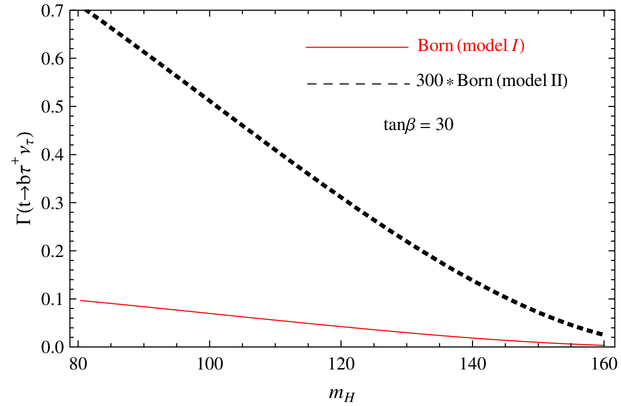

FIG. 5. As in Fig. 4 but for $\tan\beta = 30$.

where $\Gamma_0^{\textbf{Model I}} = 159\times 10^{-4}$ and $\Gamma_0^{\textbf{Model II}} = 700\times 10^{-4}$. Also, for $m_{H^+} = 85$ GeV and $\tan\beta = 8$, they read

$$\Gamma^{\textbf{Model I}}_{\rm NLO}(t \to bH^+) = \Gamma_0^{\prime\textbf{Model I}}(1 - 0.0870),$$
$$\Gamma^{\textbf{Model II}}_{\rm NLO}(t \to bH^+) = \Gamma_0^{\prime\textbf{Model II}}(1 - 0.4627), \qquad (41)$$

where $\Gamma_0^{\prime\textbf{Model I}} = 149\times 10^{-4}$ and $\Gamma_0^{\prime\textbf{Model II}} = 656\times 10^{-4}$. As is seen, the NLO QCD corrections to the decay rates are significant, especially when the type-II 2HDM scenario is concerned.

IV. INTERFERENCE EFFECTS OF AMPLITUDES

Considering the decay modes

$$t \to b + W^+/H^+(\to l^+\nu^+), \qquad (42)$$

the full amplitude for the top decay process is the sum of the amplitudes in the SM and BSM theories, i.e.,

$$M^{\rm Total}(t \to bl^+\nu^+) = M^{\rm SM}_{t\to bl^+\nu^+} + M^{\rm BSM}_{t\to bl^+\nu^+}. \qquad (43)$$

At the Born level, the matrix element squared is $|M_0|^2 = |M_0^{\rm SM}|^2 + |M_0^{\rm BSM}|^2 + 2{\rm Re}(M_0^{\rm BSM}\cdot M_0^{\rm SM\dagger})$, where the amplitudes $M_0^{\rm SM}$ and $M_0^{\rm BSM}$ are given in (2) and (29), respectively. Considering the Born decay width (7) and the phase space element (6), one can obtain the total Born decay width as

$$\Gamma_t^{\rm Tot} = \Gamma_0^{\rm SM}(t\to bl^+\nu_l) + \Gamma_0^{\rm BSM}(t\to bl^+\nu_l) + \Gamma_0^{\rm Int}, \qquad (44)$$

where $\Gamma_0^{\rm SM}$ and $\Gamma_0^{\rm BSM}$ are given in (8) and (31), respectively. In all manuscripts, it is postulated that the contribution of the interference term can be ignored while it needs some subtle accuracies. In this section, we intend to estimate this contribution at leading order, i.e., $\Gamma_0^{\rm Int}$, to show when one is allowed to omit this contribution.

The contribution of interference amplitude squared is obtained as

$$\overline{|M_0^{\rm Int}|^2} = \frac{1}{2}\sum_{\rm spin}(2{\rm Re}|M_0^{\rm BSM}.M_0^{\rm SM\dagger}|^2) = \left(\frac{g_W^2}{8m_W}|V_{tb}|\right)^2$$
$$\times \frac{(p_W^2 - m_W^2)(p_H^2 - m_H^2) + m_W m_H \Gamma_W \Gamma_H}{[(p_W^2 - m_W^2)^2 + m_W^2\Gamma_W^2][(p_H^2 - m_H^2)^2 + m_H^2\Gamma_H^2]}$$
$$\times(-64 m_l C[A m_t(p_b\cdot p_\nu) + B m_b(p_t\cdot p_\nu)]), \qquad (45)$$

where $p_t\cdot p_\nu = m_t E_\nu$ and $2p_b\cdot p_\nu = m_t^2 + m_l^2 - m_b^2 - 2m_t E_l$ in the top rest frame. The kinematic restrictions are

$$0 \le E_l \le \frac{m_t(1-R)}{2},$$
$$\frac{m_t}{2}\left(1 - R - 2\frac{E_l}{m_t}\right) \le E_\nu \le \frac{m_t}{2}\left(1 - \frac{m_t R}{m_t - 2E_l}\right). \qquad (46)$$

Finally, defining $l = (m_l/m_t)^2$, for the contribution of the interference term in the top decay rate, one has

$$\Gamma_0^{\rm Int}(t \to bl^+\nu_l) = \frac{C\alpha^2\sqrt{l}}{2^7\pi m_t^2\omega\sin^4\theta_W}\left\{2m_t(R-1)(A - B\sqrt{R}) + \frac{1}{m_t^2(y-\omega)^2 + (\sqrt{y}\Gamma_H + \sqrt{\omega}\Gamma_W)^2}[f(y,\omega,\Gamma_H,\Gamma_W)\right.$$
$$\left. + g(y,\omega,\Gamma_H,\Gamma_W) + h(y,\omega,\Gamma_H,\Gamma_W) + Q(y,\omega,\Gamma_H,\Gamma_W)]\right\}, \qquad (47)$$

where $g(y,\omega,\Gamma_H,\Gamma_W) = f(y \leftrightarrow \omega, \Gamma_H \leftrightarrow \Gamma_W)$ so that

$$f(y,\omega,\Gamma_H,\Gamma_W) = m_t \ln\frac{(R-y)^2 m_t^2 + y\Gamma_H^2}{(1-y)^2 m_t^2 + y\Gamma_H^2}(m_t^2(y-\omega)[A(1-y)^2 + B\sqrt{R}(1-y^2)] + 2\sqrt{y\omega}\Gamma_H\Gamma_W[A(y-1) - By\sqrt{R}] + y\Gamma_H^2[A(y+\omega-2) - B(y+\omega)\sqrt{R}]), \tag{48}$$

and $Q(y,\omega,\Gamma_H,\Gamma_W) = h(y\leftrightarrow\omega, \Gamma_H\leftrightarrow\Gamma_W)$, where

$$h(y,\omega,\Gamma_H,\Gamma_W) = 2\left[\tan^{-1}\frac{m_t(R-y)}{\sqrt{y}\Gamma_H} - \tan^{-1}\frac{m_t(1-y)}{\sqrt{y}\Gamma_H}\right][(B\sqrt{R}-A)(y\Gamma_W\Gamma_H^2\sqrt{\omega} + (\Gamma_H\sqrt{y})^3 + m_t^2\Gamma_H(y^2-2y\omega+1)\sqrt{y} - m_t^2(y^2-1)\Gamma_W\sqrt{\omega}) + 2Am_t^2((1-\omega)\Gamma_H\sqrt{y} + (1-y)\Gamma_W\sqrt{\omega})]. \tag{49}$$

In the above relations, $\Gamma_W = 2.085$ [30], and concentrating on $l^+ = \tau^+$, one has $\Gamma_H = \Gamma(H^+\to\tau^+\nu_\tau) + \Gamma(H^+\to c\bar{s})$, which are given in (36) and (37) for models I and II.

In Figs. 6–8, we studied the dependence of the interference term on $\tan\beta$ considering $m_{H^+} = m_{W^+}$ (in Fig. 6), $m_{H^+} = 85$ GeV (in Fig. 7), and $m_{H^+} = 120$ GeV (in Fig. 8). As is seen, for $m_{H^+} = m_{W^+}$, this contribution in model I is positive for all values of $\tan\beta$, while this is negative in model II. This behavior is vice versa in Fig. 8, in which we set $m_H = 120$ GeV. For $\tan\beta > 2$, the absolute value of interference contribution in model II is always larger than the one in model I.

In Figs. 9 and 10, we investigate the dependence of the interference term on the charged Higgs mass by fixing $\tan\beta = 8$ (in Fig. 9) and $\tan\beta = 30$ (in Fig. 10). As is seen, the maximum value of the interference contribution occurs for $m_{H^+} \approx m_{W^+}$, and it goes to zero when $\tan\beta$ increases. To work out our conclusion, here, we concentrate on the two following examples:

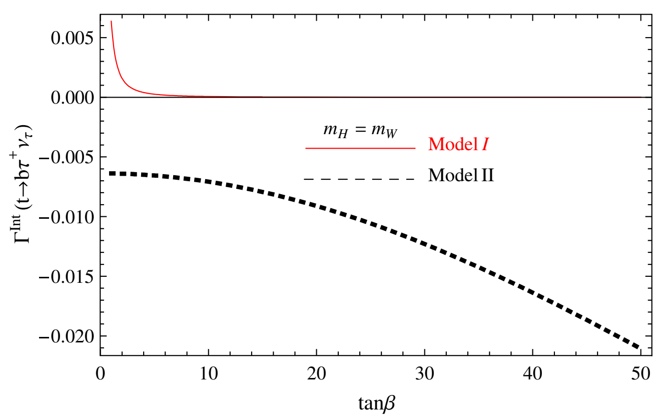

FIG. 6. The interference contribution as a function of $\tan\beta$ for which we fixed the Higgs mass as $m_{H^+} = m_{W^+}$.

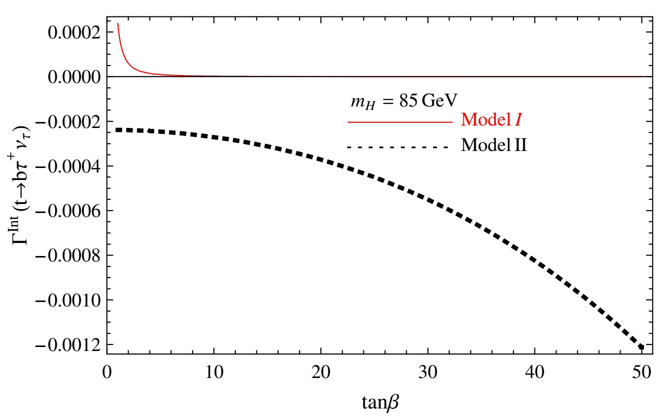

FIG. 7. As in Fig. 6 but for $m_{H^+} = 85$ GeV.

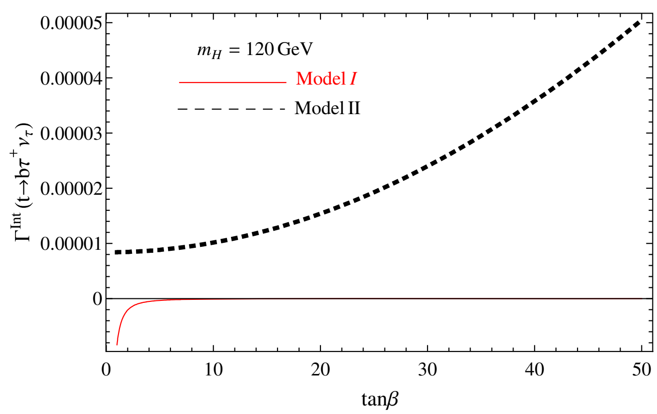

FIG. 8. As in Fig. 6 but for $m_{H^+} = 120$ GeV.

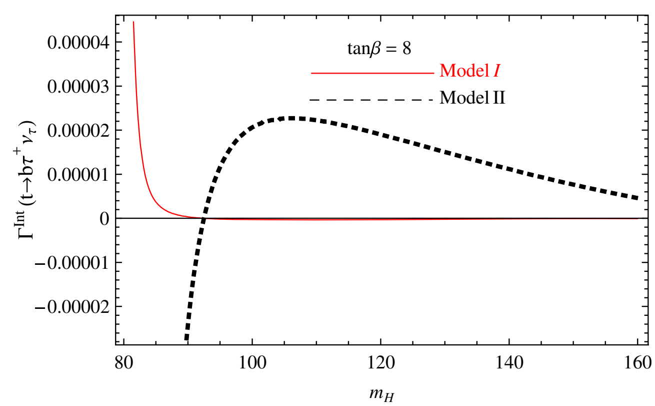

FIG. 9. The contribution of interference term in the Born decay rate of $t\to b\tau^+\nu_\tau$ as a function of m_{H^+} in two scenarios for which $\tan\beta = 8$ is set.

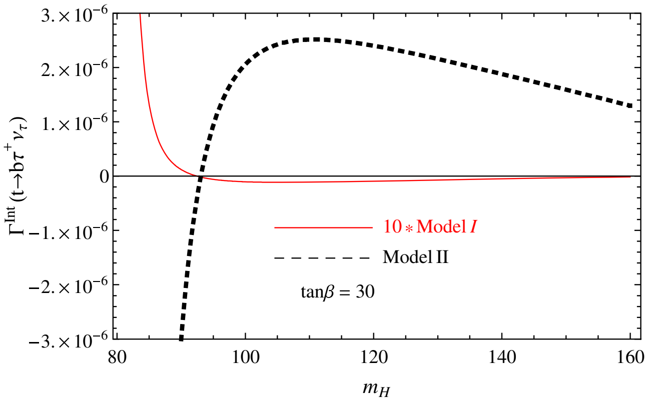

FIG. 10. As in Fig. 9 but for $\tan\beta = 30$.

(1) Taking $m_{H^+} \approx m_{W^+}$ and $\tan\beta = 8$, in the type-I 2HDM, one has

$$\Gamma^{\rm Total}_{\rm NLO}(t\to b\nu^+\nu_\tau) = \Gamma^{\rm SM}_0(1-0.0853) + \Gamma^{{\rm BSM},I}_0(1-0.0879) + \Gamma^{\rm Int}, \tag{50}$$

where $\Gamma^{\rm SM}_0 = 0.1543$, $\Gamma^{{\rm BSM},I}_0 = 4.53\times10^{-3}$, and the interference contribution at lowest order reads $\Gamma^{\rm Int}_0 =$ 9.95×10^{-5}. This result in the type-II 2HDM reads

$$\Gamma^{\rm Total}_{\rm NLO}(t\to b\nu^+\nu_\tau) = \Gamma^{\rm SM}_0(1-0.0853) + \Gamma^{{\rm BSM},II}_0(1-0.463) + \Gamma^{\rm Int}, \tag{51}$$

where $\Gamma^{{\rm BSM},II}_0 = 6.94\times10^{-2}$ and the interference contribution reads $\Gamma^{\rm Int}_0 = -6.82\times10^{-3}$. This example shows that the interference contribution in the type-I and -II scenarios is about 2% and −9% of the contribution from 2HDM at leading order (LO), respectively.

(2) Taking $m_{H^+} = 85$ GeV and $\tan\beta = 8$, in the type-I 2HDM, one has

$$\Gamma^{\rm Total}_{\rm NLO}(t\to b\nu^+\nu_\tau) = \Gamma^{\rm SM}_0(1-0.0853) + \Gamma^{{\rm BSM},I}_0(1-0.870) + \Gamma^{\rm Int}, \tag{52}$$

where $\Gamma^{{\rm BSM},I}_0 = 4.2\times10^{-3}$ and the interference contribution at LO reads $\Gamma^{\rm Int}_0 = 9.2\times10^{-6}$. This result in the type-II 2HDM reads

$$\Gamma^{\rm Total}_{\rm NLO}(t\to b\nu^+\nu_\tau) = \Gamma^{\rm SM}_0(1-0.0853) + \Gamma^{{\rm BSM},II}_0(1-0.462) + \Gamma^{\rm Int}, \tag{53}$$

where $\Gamma^{{\rm BSM},II}_0 = 0.0651$ and the interference term is $\Gamma^{\rm Int}_0 = -129\times10^{-6}$.

These two examples show that for $m_{H^+} \approx m_{W^+}$ the contribution of interference term, specifically in the type-II 2HDM, is considerable and its value cannot be ignored.

Therefore, our numerical results emphasize that if the mass gap between two intermediate particles (W^+ and H^+ in our work) is smaller than one of their total widths, the interference term between the contributions from the two nearly mass-degenerate particles may become considerable. In other words, the interference effects can be considerable if there are several resonant diagrams of which the intermediate particles (in general, with masses M_1 and M_2 for two resonances) are close in mass compared to their total decay widths: $|M_1 - M_2| \le (\Gamma_1, \Gamma_2)$ [31]. In these situations, a single resonance approach or the incoherent sum of two resonance contributions does not necessarily hold, and it needs more attention. In fact, if the mass difference is smaller than their total widths, the two resonances overlap. This can lead to a considerable interference term, which was neglected in the standard NWA but can be taken into account in the full calculation or in a generalized NWA [31].

V. CONCLUSIONS

In a general 2HDM, the main production mode of a light charged Higgs bosons (with $m_{H^+} \le m_t$) is through the top quark decay, $t\to bH^+$, followed by $H^+\to\tau^+\nu_\tau$. In this work, we have calculated the total decay rate of the top quark, i.e., $t\to b+W^+/H^+\to bl^+\nu_l$, at the standard model of particle physics as well as the 2HDM theory. In the first part of our work, we calculated the Born decay rate for the full process in which one deals with the stable intermediate bosons W^+ and H^+. Extension of this procedure to higher orders of perturbative QED/QCD is complicated, but it would be possible using the narrow-width approximation for particles having a total width much smaller than their masses. Next, using the NWA, we recalculated the aforementioned decay rates and showed that the accuracy of NWA is about (2–5)%. Within this approach, we presented our numerical analysis at NLO.

A necessary and important condition limiting the applicability of NWA is the requirement that there should be no interference of the contribution of the intermediate particle for which the NWA is applied with any other close-by resonance. While within the SM of particle physics this condition is usually valid for relevant processes at high-energy colliders such as the CERN LHC or a future linear collider, many models of physics beyond the SM have mass spectra in which two or more states can be nearly mass degenerate. If the mass gap between two intermediate particles is smaller than one of their total widths, their resonances overlap, so the interference contribution cannot be neglected if the two states mix.

In the last section of our paper, we investigated the interference effect of two intermediate particles in top decay, i.e., W^+ and H^+ bosons, and showed when this effect is considerable and the NWA is insufficient. Our results confirmed that when the mass of charged Higgs boson is considered equal or near to the W^+ mass (referred to as nearly mass-degenerate particles) the interference effects are sizable and considerable, specifically for the type-II 2HDM. For larger values of m_{H^+} this contribution can be omitted with high accuracy. It should be pointed out that several cases have been already identified in the literature in which the NWA is insufficient due to sizable interference effects, e.g., in the context of the MSSM in Refs. [49,50] and in the context of two- and multiple-Higgs models and in Higgsless models in Ref. [51].

[1] S. Moch and P. Uwer, Nucl. Phys. B, Proc. Suppl. **183**, 75 (2008).
[2] S. Moch and P. Uwer, Phys. Rev. D **78**, 034003 (2008).
[3] N. Kidonakis and R. Vogt, Phys. Rev. D **78**, 074005 (2008).
[4] M. Cacciari, S. Frixione, M. L. Mangano, P. Nason, and G. Ridolfi, J. High Energy Phys. 09 (2008) 127.
[5] A. Ali and E. Pietarinen, Nucl. Phys. **B154**, 519 (1979).
[6] G. Corbo, Nucl. Phys. **B212**, 99 (1983).
[7] G. Altarelli, N. Cabibbo, G. Corbo, L. Maiani, and G. Martinelli, Nucl. Phys. **B208**, 365 (1982).
[8] M. Ježabek and J. H. Kühn, Nucl. Phys. **B320**, 20 (1989).
[9] A. Czarnecki, Phys. Lett. B **252**, 467 (1990).
[10] J. a. Liu and Y. P. Yao, Int. J. Mod. Phys. A **6**, 4925 (1991).
[11] C. S. Li, R. J. Oakes, and T. C. Yuan, Phys. Rev. D **43**, 3759 (1991).
[12] M. Fischer, S. Groote, J. G. Körner, and M. C. Mauser, Phys. Rev. D **63**, 031501 (2001).
[13] B. A. Kniehl, G. Kramer, and S. M. Moosavi Nejad, Nucl. Phys. **B862**, 720 (2012).
[14] S. M. Moosavi Nejad, Phys. Rev. D **88**, 094011 (2013).
[15] S. M. Moosavi Nejad, Nucl. Phys. **B905**, 217 (2016).
[16] S. M. Moosavi Nejad and M. Balali, Eur. Phys. J. C **76**, 173 (2016).
[17] S. M. Moosavi Nejad and M. Balali, Phys. Rev. D **90**, 114017 (2014); **93**, 119904(E) (2016).
[18] T. D. Lee, Phys. Rev. D **8**, 1226 (1973).
[19] A. Djouadi, Phys. Rept. **459**, 1 (2008).
[20] J. F. Gunion and H. E. Haber, Nucl. Phys. **B272**, 1 (1986); **B402**, 567(E) (1993).
[21] C. Degrande, R. Frederix, V. Hirschi, M. Ubiali, M. Wiesemann, and M. Zaro, Phys. Lett. B **772**, 87 (2017).
[22] C. S. Li and R. J. Oakes, Phys. Rev. D **43**, 855 (1991).
[23] A. Czarnecki and S. Davidson, Phys. Rev. D **48**, 4183 (1993).
[24] J. G. Körner and M. C. Mauser, Eur. Phys. J. C **54**, 175 (2008).
[25] S. M. Moosavi Nejad, Phys. Rev. D **85**, 054010 (2012).
[26] S. M. Moosavi Nejad, Eur. Phys. J. C **72**, 2224 (2012).
[27] S. M. Moosavi Nejad and S. Abbaspour, Nucl. Phys. **B921**, 86 (2017).
[28] F. Kling, A. Pyarelal, and S. Su, J. High Energy Phys. 11 (2015) 051.
[29] N. Cabibbo, Phys. Rev. Lett. **10**, 531 (1963); M. Kobayashi and T. Maskawa, Prog. Theor. Phys. **49**, 652 (1973).
[30] C. Patrignani *et al.* (Particle Data Group), Chin. Phys. C **40**, 100001 (2016).
[31] E. Fuchs, S. Thewes, and G. Weiglein, Eur. Phys. J. C **75**, 254 (2015).
[32] J. Beringer *et al.* (Particle Data Group), Phys. Rev. D **86**, 010001 (2012).
[33] G. Eilam, R. R. Mendel, R. Migneron, and A. Soni, Phys. Rev. Lett. **66**, 3105 (1991).
[34] A. Arbuzov, D. Bardin, S. Bondarenko, P. Christova, L. Kalinovskaya, G. Nanava, R. Sadykov, and W. von Schlippe, Eur. Phys. J. C **51**, 585 (2007).
[35] B. K. Bullock, K. Hagiwara, and A. D. Martin, Phys. Rev. Lett. **67**, 3055 (1991).
[36] A. Ali, E. A. Kuraev, and Y. M. Bystritskiy, Eur. Phys. J. C **67**, 377 (2010).
[37] B. Abbott *et al.* (D0 Collaboration), Phys. Rev. Lett. **82**, 4975 (1999).
[38] A. Abulencia *et al.* (CDF Collaboration), Phys. Rev. Lett. **96**, 042003 (2006).
[39] G. Aad *et al.* (ATLAS Collaboration), J. Instrum. **3**, P07007 (2008).
[40] V. D. Barger, J. L. Hewett, and R. J. N. Phillips, Phys. Rev. D **41**, 3421 (1990).
[41] K. Inoue, A. Kakuto, H. Komatsu, and S. Takeshita, Prog. Theor. Phys. **68**, 927 (1982); **70**, 330(E) (1983).
[42] P. Fayet, Nucl. Phys. **B90**, 104 (1975).
[43] S. Raychaudhuri and D. P. Roy, Phys. Rev. D **52**, 1556 (1995).
[44] G. Aad *et al.* (ATLAS Collaboration), J. High Energy Phys. 06 (2012) 039.
[45] G. Aad *et al.* (ATLAS Collaboration), J. High Energy Phys. 03 (2013) 076.
[46] G. Aad *et al.* (ATLAS Collaboration), Eur. Phys. J. C **73**, 2465 (2013).
[47] V. Khachatryan *et al.* (CMS Collaboration), J. High Energy Phys. 11 (2015) 018.
[48] V. Khachatryan *et al.* (CMS Collaboration), J. High Energy Phys. 12 (2015) 178.
[49] D. Berdine, N. Kauer, and D. Rainwater, Phys. Rev. Lett. **99**, 111601 (2007).
[50] J. Kalinowski, W. Kilian, J. Reuter, T. Robens, and K. Rolbiecki, J. High Energy Phys. 10 (2008) 090.
[51] G. Cacciapaglia, A. Deandrea, and S. De Curtis, Phys. Lett. B **682**, 43 (2009).